

# Non standard analysis of the solar neutrino anomaly

(updated on July 2001 including the SNO CC data\*)  
 (updated on July 2002 including the SNO day/night spectral CC and NC data<sup>†</sup>)

**Riccardo Barbieri**

*Scuola Normale Superiore, Piazza dei Cavalieri 7, I-56126 Pisa, Italy and INFN*

**Alessandro Strumia**

*Theory division, CERN and Dipartimento di Fisica, Università di Pisa and INFN*

## Abstract

Continuing previous work, a model independent analysis of the solar neutrino anomaly is performed in terms of neutrino oscillations, allowing a comparison with the predictions of the Standard Solar Model. SMA and LMA solutions emerge also in this case, although somewhat different from the standard ones. The significance of the NC/CC double ratio measurable in SNO is illustrated in this context.

## 1 Introduction and motivations

Flavour neutrino oscillations continue to be a pretty controversial matter. It is fair to recall that, so far, no direct signal of them, like neutrino appearance or explicit oscillation patterns, have been observed either in solar or in atmospheric neutrinos. The up/down asymmetry of the flux of the atmospheric  $\nu_\mu$  and  $\bar{\nu}_\mu$  neutrinos gives, however, an indisputable evidence for the presence of an atmospheric neutrino anomaly. No equally clear evidence has been found, on the other hand, for the solar neutrino anomaly [1, 2, 3, 4], since its standard interpretation relies on a combination of many different experimental and theoretical ingredients. Furthermore, the LNSD result still awaits for an independent confirmation.

On the solar neutrinos, which are the subject of this paper, quite different attitudes can be taken, depending on the weight one gives to the input of the Standard Solar Model (SSM) [5]. On one side, it does not look reasonable to consider the solar neutrino anomaly as an artifact due to a large unknown error in solar models or in solar neutrino experiments. The other extreme attitude is to assume that all the ingredients of the analysis are correct, thus obtaining a rather precise determi-

nation of the neutrino oscillation parameters. As well known, the best fits of the solar neutrino deficit in this framework are given by few peculiar energy-dependent survival probabilities.

The truth is that unfortunately, so far, SuperKamio- kande (SK) has not found any evidence for a distortion of the energy spectrum, nor for Earth regeneration effects, nor for seasonal variations of the neutrino flux. Furthermore, the most recent SK data [2, 4] worsen the quality of the best fit, with the net result that the new best fit regions now include values of the oscillation parameters previously discarded on the basis of the sole neutrino rates. Recent analyses found that all the distinct best fit solutions have a high goodness-of-fit probability [6]. However, at least in part, this is just a reflection of having fitted the few really problematic data together with many other ‘degrees of freedom’ that have not much to do with the problem. To really judge the quality of the fit one should perform a more complete statistical analysis or rewrite the data in terms of a minimal set of ‘optimal’ observables\*.

In view of this situation, we find it useful to come back to an analysis which has minimal dependence upon the SSM inputs. This is the purpose of this paper,

\*The addendum at page 9 (section 5) is not present in the published version of this paper.

<sup>†</sup>The addendum at page 10 (section 6) is not present in the published version of this paper.

\*A similar comment can be done for atmospheric neutrinos. It is hard to judge if the  $\nu_\tau \rightarrow \nu_{\text{sterile}}$  interpretation gives an acceptable fit by looking only at the minimal  $\chi^2$  of a global fit that includes electron data, low energy data and too many zenith angle bins.

continuing previous work along similar lines. From an experimental point of view, the main new information comes from the SK measurements, mentioned above, of the energy spectrum and of day/night or seasonal variations of the neutrino flux. Their interpretation has little to do with the theoretical input of the SSM.

The SSM independent analysis is performed in section 2. In section 3 we discuss its implications for new solar experiments. Conclusions are drawn in section 4. In appendix A we describe the details of the computation. In appendix B we discuss how KamLand and neutrino factories can test a high value of  $\Delta m_{12}^2 \gtrsim 10^{-4} \text{ eV}^2$ , allowed by solar data in presence of an undetected systematic error in the Chlorine experiment.

Fitting the solar, atmospheric and LSND anomalies with neutrino oscillations consistently with all bounds would require more than 3 neutrinos and peculiar models. We limit ourselves to oscillations between the 3 SM active neutrinos and we await for a confirmation of the LSND result [7], disregarded in the following. We use the same notations as in [8]. The three neutrino masses  $m_i$  are ordered such that  $\Delta m_{23}^2 > \Delta m_{12}^2 > 0$  where  $\Delta m_{ij}^2 \equiv m_j^2 - m_i^2$ . The neutrino mixing matrix is parameterized as

$$V = R_{23}(\theta_{23}) \text{diag}(1, e^{i\phi}, 1) R_{13}(\theta_{13}) R_{12}(\theta_{12}) \quad (1)$$

where  $R_{ij}(\theta_{ij})$  represents a rotation by  $\theta_{ij}$  in the  $ij$  plane,  $0 \leq \theta_{ij} \leq \pi$ , and  $\phi$  is a CP-violating phase. With these notations,  $\theta_{23}$  and  $\Delta m_{23}^2 \approx \Delta m_{13}^2$  are relevant to the atmospheric neutrino anomaly,  $\theta_{12}$  and  $\Delta m_{12}^2$  to the solar anomaly, while  $\theta_{13}$  can affect both solar and atmospheric neutrinos.

## 2 SSM independent analysis

One can perform a *useful* almost SSM independent analysis [9, 8] by just treating the overall  $^8\text{B}$  and  $^7\text{Be}$  fluxes as unknown quantities, to be extracted from the data. Here we briefly recall how this procedure is justified (see [8] for explanations and references). First, it is safe to use the standard spectral functions for the energy distributions of the single components

$$i = \{\text{pp}, \text{pep}, ^7\text{Be}, ^{13}\text{N}, ^{15}\text{O}, ^{17}\text{F}, ^8\text{B}, \text{hep}\}$$

of the solar neutrino flux, while the total flux  $\Phi_i$  of each component is regarded as unknown. Second, it is safe to set to their standard values the ratios  $\Phi_{^{13}\text{N}}/\Phi_{^{15}\text{O}}$  and  $\Phi_{\text{pep}}/\Phi_{\text{pp}}$ , to neglect  $^{17}\text{F}$  neutrinos and to consider hep neutrinos only when computing the upper tail of the energy spectrum of recoil electrons in SK. Although to a somewhat lesser extent, it is also safe to set  $\Phi_{^{13}\text{N}}/\Phi_{^7\text{Be}}$

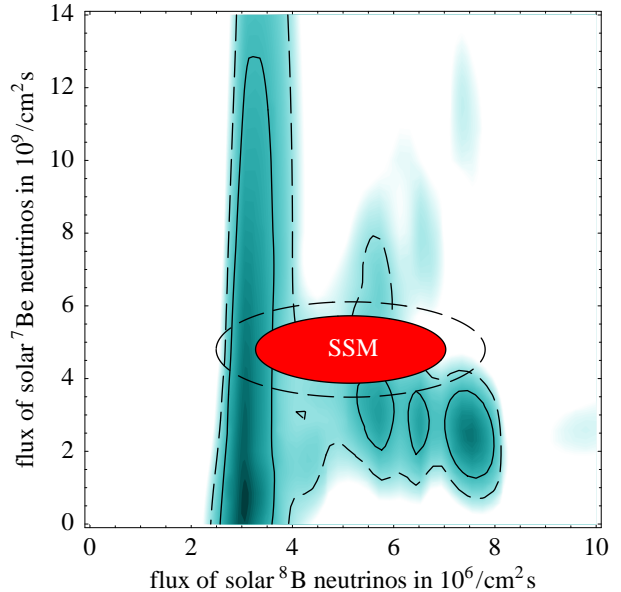


Figure 1: *Best fit values of the neutrino solar fluxes, as obtained by this analysis, compared with SSM theoretical predictions.*

to its standard value. Finally the solar luminosity constraint allows to express the pp flux in terms of the remaining free parameters  $\Phi_{^7\text{Be}}$  and  $\Phi_{^8\text{B}}$ .

This kind of analysis is useful because solar neutrino rates have been measured by *three* different kinds of experiments. For any given oscillation pattern, each measured rate gives an allowed band in the  $(\Phi_{^8\text{B}}, \Phi_{^7\text{Be}})$  plane (few examples are shown in fig. 2). Requiring a crossing of all the three experimental bands selects specific oscillation patterns. In this way one converts experimental data into informations on the oscillation parameters *and* on the neutrino fluxes  $\Phi_{^8\text{B}}$  and  $\Phi_{^7\text{Be}}$ . This kind of analysis will become more powerful when the SNO and Borexino experiments will present their data. Already now the results are much more restrictive than two years ago [8]. SK and Gallium experiments have measured more precisely their fluxes and the new SK data now exclude in a SSM independent way a large part of the oscillation parameter space where MSW effects are large.

Furthermore, the CHOOZ bound on  $\bar{\nu}_e$  disappearance [10] now holds for all values of the mass splitting  $\Delta m_{13}^2$  allowed by the SK atmospheric data. This was not the case one year ago, and implies that  $\theta_{13}$  is small,  $\theta_{13} < 15^\circ$  at 95% C.L. Therefore  $\theta_{13}$  can only have a minor impact on solar neutrino experiments. Unless otherwise indicated we will assume that  $\theta_{13} = 0$ .

The best-fit values of the neutrino fluxes  $\Phi_{^8\text{B}}$  and  $\Phi_{^7\text{Be}}$  are shown in fig. 1. The regions delimited by con-

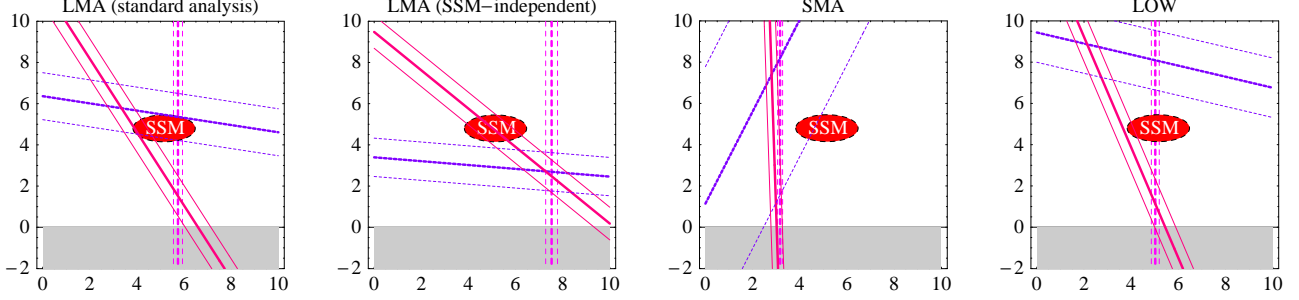


Figure 2: Values of the solar neutrino fluxes ( $\Phi_{sB}, \Phi_{7Be}$ ) measured by the Chlorine experiment (continuous lines), the Gallium experiment (dashed lines) and by the SuperKamiokande experiment (long dashed lines) assuming four neutrino oscillation schemes: • the standard best-fit LMA point in fig. 2a; • the solar-model independent best-fit LMA point in fig. 2b; • the best-fit SMA point in fig. 2c; • the best-fit LOW point in fig. 2d. All four plots have the flux of  $^8B$  neutrinos in  $10^6 \text{ cm}^{-2}\text{s}^{-1}$  on the horizontal axis and the flux of  $^7Be$  neutrinos in  $10^9 \text{ cm}^{-2}\text{s}^{-1}$  on the vertical axis. The ellipse is the Standard Solar Model prediction. All errors correspond to one standard deviation.

tinuous (dashed) lines give the best fit at 90% (99%) C.L.<sup>†</sup> The ellipses represent the 90% and 99% C.L. SSM prediction for these fluxes [5]:

$$\Phi_{sB}|_{\text{SSM}} = 5.15 (1_{-0.14}^{+0.19}) \cdot 10^6 / \text{cm}^2\text{s}, \quad (2a)$$

$$\Phi_{7Be}|_{\text{SSM}} = 4.8(1 \pm 0.09) \cdot 10^9 / \text{cm}^2\text{s} \quad (2b)$$

A standard analysis would include these theoretical constraints in the  $\chi^2$ , forcing  $\Phi_{sB}$  and  $\Phi_{7Be}$  to be close to the SSM predictions.

Fig. 1 shows that the best fit regions are neither far from the SSM predictions of eq. (2) nor peaked around them. This reflects the fact that oscillation patterns that gave the best standard fits of the measured neutrino rates are now disfavoured by the SK SSM-independent data. Basically there are two distinct best-fit regions in fig. 1:

- A region with  $\Phi_{sB} > 5 \cdot 10^6 / \text{cm}^2\text{s}$  and  $\Phi_{7Be} < 5 \cdot 10^9 / \text{cm}^2\text{s}$  produced by values of the mixing parameters around the LMA solution. Fig. 2b shows how a perfect crossing of the three experimental bands occur around  $\Phi_{sB} \approx 7.5 \cdot 10^6 / \text{cm}^2\text{s}$  and  $\Phi_{7Be} \approx 3 \cdot 10^9 / \text{cm}^2\text{s}$ . This crossing is obtained for  $\Delta m_{12}^2 = 4 \cdot 10^{-5} \text{ eV}^2$  and  $\theta_{12} = 0.42$ . The standard analysis requires a crossing centered around

<sup>†</sup>The contour lines are drawn at  $\Delta\chi^2$  levels that correspond to 90% and 99% C.L., if one converts values of  $\Delta\chi^2$  into “best fit probabilities”  $p$  using the standard expressions valid for a gaussian probability distribution. This is not a good approximation since, as frequently happens in solar neutrino fits, one finds few separate best-fit solutions, while a gaussian would have only one peak. A proper treatment would shift the values of  $1-p$  by relative  $\mathcal{O}(1)$  factors. A comparable shift would arise if we performed an exact marginalization of the joint probability distribution with respect to the oscillation parameters. We neglect such corrections, since they are comparable to the uncertainties of Bayesian inference arising from the need of choosing some prior distribution function.

the SSM prediction: the best fit is obtained for a slightly larger values of  $\theta_{12}$  and gives the worse crossing shown in fig. 2a.

- A region with  $\Phi_{sB} \in [2.5 \dots 4] \cdot 10^6 / \text{cm}^2\text{s}$  produced by values of the mixing parameters around the SMA solution. The best crossing, obtained for  $\theta_{12} = 0.025$  and  $\Delta m_{12}^2 = 0.5 \cdot 10^{-5} \text{ eV}^2$  is shown in fig. 2c. It also gives the best standard fit. The previous best standard fit had larger  $\theta_{12} = 0.04$  and gave a crossing perfectly centered on the SSM prediction (see fig. 1c in [8]), but is incompatible with the day/night and spectral SK data.

Oscillation patterns around the LOW region (i.e. the one with large  $\theta_{12}$  and  $\Delta m^2 \lesssim 10^{-7} \text{ eV}^2$ ) give a modest fit with  $\Phi_{sB} \approx (4 \div 5) \cdot 10^6 / \text{cm}^2\text{s}$  (see fig. 2d).

Before going on, it is useful to consider the region around  $\Phi_{sB} \approx 3 \cdot 10^6 / \text{cm}^2\text{s}$  and  $\Phi_{7Be} \approx 0$ . This region appears due to a unfortunate weakness of our SSM-independent analysis: assuming no oscillations, the three bands perfectly cross at  $\Phi_{sB} \approx 3 \cdot 10^6 / \text{cm}^2\text{s}$  and  $\Phi_{7Be}$  slightly negative. Therefore the no-oscillation case cannot be excluded at a high confidence level and various oscillations patterns not much different from the no-oscillation case provide acceptable fits. We consider such crossings as unfortunate accidents. Before fitting the mixing angles, we exclude by hand such cases by imposing  $\Phi_{sB} > 0$  and  $\Phi_{7Be} > 1.5 \cdot 10^9 / \text{cm}^2\text{s}$  rather than  $\Phi_{7Be} > 0$ . This does not conflict much with our purpose of performing a SSM-independent analysis, since very low values of the  $^7Be$  flux are unphysical, as the Boron neutrinos, seen in SK, originate from the Berillium ones to a large extent.

Fig. 3 shows the fit in the usual plane of the mixing

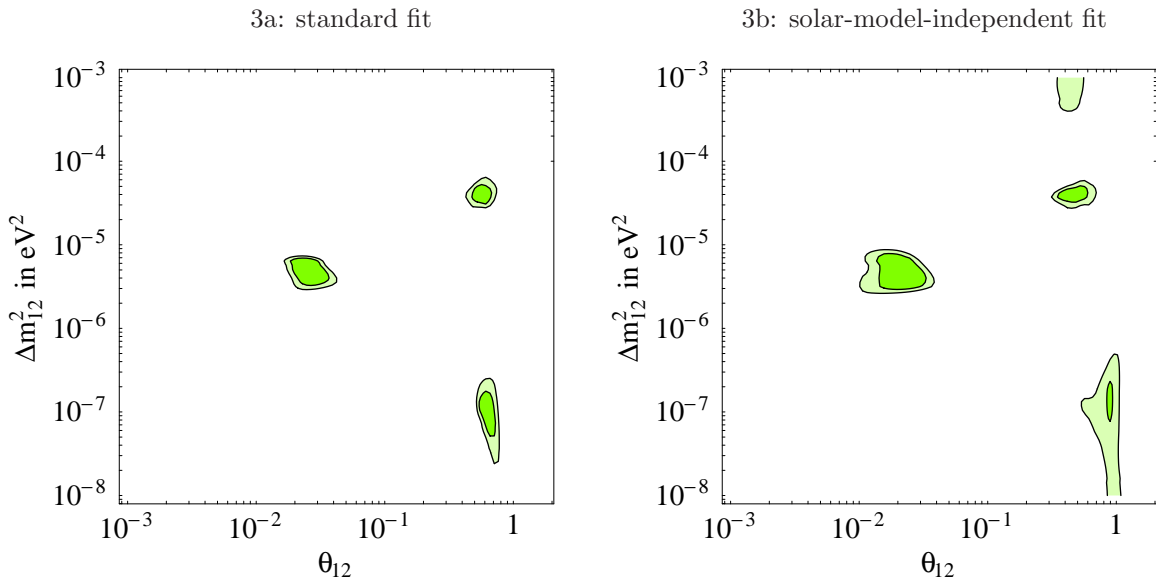


Figure 3: *Best fit value of the oscillation parameters (a) standard fit (b) solar-model-independent fit.*

parameters  $\theta_{12}$  and  $\Delta m_{12}^2$ : the standard fit is shown in fig. 3a and the solar-model independent fit in fig. 3b. The best fit regions are not entirely restricted to  $\theta_{12} < \pi/4$  [11].

Concerning the standard fit, we mention an important detail not immediately apparent from the figure. Like other standard fits [6], our fit still contains a SMA region, even if the SK spectrum and day/night data have excluded the ‘old SMA’ region with larger  $\theta_{12}$ . The ‘old SMA’ gave such a good standard fit of solar rates that values of  $\theta_{12}$  previously regarded as ‘too small’ now give an acceptable standard fit of solar rates. This is why we obtain a new best-fit SMA region, more SMA than the old one (see fig. 4a). Fig. 2c explains why such smaller values of  $\theta_{12}$  were discarded in old standard fits but not in old SSM-independent fits: they give a good crossing of the three experimental bands, but at a value of the Boron flux smaller than the one predicted by the SSM. This means that the SK spectrum and day/night data are not a problem for the solar-model independent SMA region.<sup>‡</sup> Non-zero values of  $\theta_{13}$  just below the CHOOZ bound slightly shift the crossing point towards higher Boron fluxes, and therefore slightly improve the quality of the standard fit in the SMA region.

Presently the LOW solution gives a better standard fit than the SMA solution [6]. Fig. 2d shows how the three experimental bands cross in the case of the ‘best

<sup>‡</sup>This discussion implies that the sterile neutrino interpretation of the solar neutrino anomaly is disfavoured by SK only if one imposes the SSM value of the Boron flux.

standard fit’ LOW solution,  $\theta_{12} = 0.66$  and  $\Delta m_{12}^2 = 0.8 \cdot 10^{-7} \text{ eV}^2$ . The crossing is not good, but roughly centered on the SSM prediction. A solar-model independent analysis does not reward this property. The best SSM-independent fit in the LOW region has larger  $\theta_{12}$  and lower  $\Phi_{7\text{Be}}$  than in the standard fit.

The band corresponding to the Ga experiment in fig. 2d (the almost horizontal one) is not unacceptably high because Earth-regeneration effects strongly affect neutrinos with energies  $E_\nu \approx \text{MeV} (\Delta m^2 / 4 \cdot 10^{-7} \text{ eV}^2)$ . Unfortunately radiochemical experiments, which detect such neutrinos, cannot study day/night effects. Earth-regeneration gives a  $\lesssim 10\%$  seasonal variation of the capture rate in GNO, since at Gran Sasso nights are longer in winter than in summer [12]. Gallex does not see such an effect. Present data from all Gallium experiments could be sensitive to a 10% seasonal variation.

### 3 Expectations for SNO

The fact that the SMA solution has migrated toward smaller values of  $\theta_{12}$ , previously considered only in SSM-independent analyses [8], has significant implications for the SNO experiment. Previous studies of the significance of the SNO experiment [13] found that only a global fit of various SNO precision observables could eventually discriminate between the SMA and the LMA solutions.

On the contrary, we think that it is quite possible at

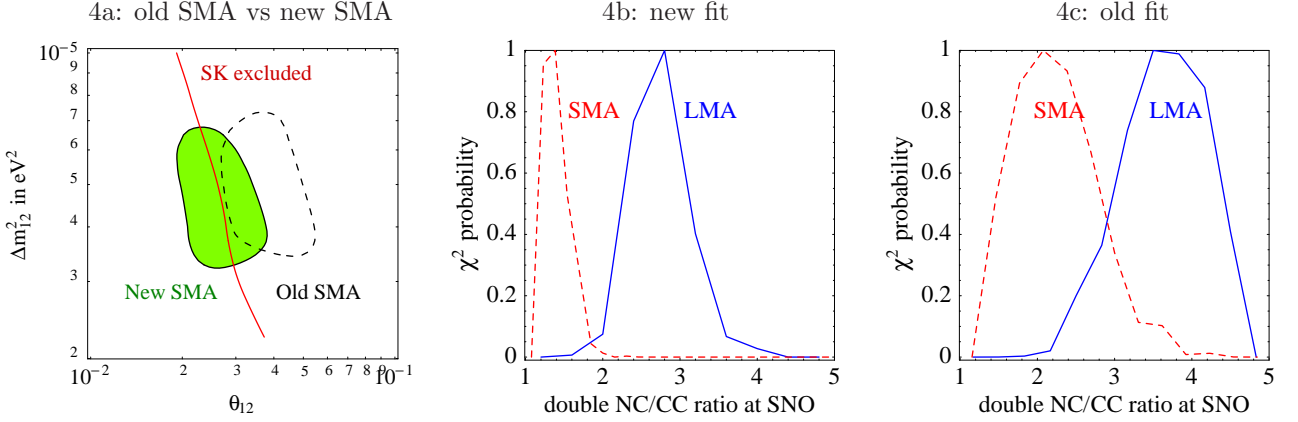


Figure 4: Fig 4a: how the SK bounds on spectral and day/night effects (continuous line) shift the best-fit SMA region: the dashed area shows the old SMA, the gray area the new SMA. All lines correspond to best fit-bounds at 90% C.L. Fig.s 4b,c show the probability distributions (see text) for the double NC/CC ratio in the new (fig. 4b) and old (fig. 4c) SMA and LMA best fit regions.

SNO to discriminate between the new LMA and the new SMA solution<sup>§</sup> or even find evidence for oscillation patterns suggested by our solar-model independent analysis by making use of the NC/CC double ratio

$$r \equiv \frac{(\text{NC rate})/(\text{CC rate})}{(\text{NC rate})/(\text{CC rate})_{\text{no oscillation}}}.$$

$r$  is an interesting observable because dominant theoretical uncertainties cancel out when taking the double ratio, and because expected oscillation effects can be very large so that one does not need a very precise determination.

In order to perform a quantitative analysis, we compute the values of  $r$  and of the  $\chi^2$ -probability

$$p \equiv \exp(-\Delta\chi^2/2)$$

for a grid of oscillation patterns in the SMA and in the LMA regions. The  $\Delta\chi^2$  is computed with respect to the local LMA or SMA minimal  $\chi^2$ , so that  $p = 1$  in the best-fit SMA point and in the best-fit LMA point. We assume an energy threshold  $T_e > 5$  MeV on the recoil electrons originating from CC interactions  $\nu_e d \rightarrow ppe$ , but our final results do not depend on this choice.

In fig. 4b,c we plot  $p(r)$ , the maximal value of  $p$  at which any value of  $r$  can be reached in the LMA and in the SMA region. The  $\chi^2$  is computed performing a standard analysis. In fig. 4b we have included the most recent SK data, while in fig. 4c we have not included them. Fig. 4b shows that there is now a neat separation between SMA and LMA predictions: measuring  $r < 2$  or  $r > 2$  would have clear implications. A measurement of  $r$  can also provide a signal for non standard solutions.

<sup>§</sup>This observation was also made in a recent paper [14].

Dividing the possible values of  $r$  in 5 distinct ranges, we can summarize the situation in the following way:

1. values of  $r$  very close to 1 are allowed in the non standard part of the SSM-independent SMA region (with smaller  $\theta_{12}$  and low  $^8\text{B}$  flux). Oscillations into sterile neutrinos would also give  $r = 1$ .
2.  $1 < r < 2$  is allowed in the standard or SSM-independent SMA region.
3.  $r$  very close to 2 is the value predicted by the non standard solution with high  $\Delta m_{12}^2$  and  $\theta_{12} \approx \pi/4$  [8, 15], allowed in presence of an undetected systematic error in the Chlorine experiment.
4.  $2 < r < 4$  is allowed in the standard or SSM-independent LMA region;
5.  $4 < r < 5$  is still allowed in the non standard part of the LMA region;

For completeness it should be said that values of  $r$  between 1.5 and 3 are expected also in the standard LOW region.

The SNO experiment will improve also the experimental knowledge of the solar neutrino fluxes. The NC rate is not affected by oscillations between active neutrinos, and therefore provides a measurement of the Boron flux. It is expected to have a  $\lesssim 10\%$  systematic error, mainly due to the uncertainty in the detection cross section [13]. Due to the large spread between the values of the Boron flux required by the different oscillation patterns (see fig. 1) this measurement will also have a significant impact. In particular the SMA solution requires low values of the Boron flux.

The Borexino experiment will be mainly sensitive to the Berillium component of the solar neutrino flux. Therefore its data will be represented by one quasi-horizontal band in fig.s 2, at a level dependent on the actual oscillation pattern. Although the main features can be seen already from fig.s 1 and 2, a true understanding of the impact of Borexino data on a SSM-independent analysis will require a combined fit of the oscillation parameters and of the neutrino fluxes.

The KamLand reactor experiment [21] will measure accurately the oscillation parameters, if they lie in the LMA region (see fig. 6). In this case, the solar neutrino data will give the  $^8\text{B}$  and  $^7\text{Be}$  solar fluxes. In particular, the Borexino data will be crucial for an accurate determination of the  $^7\text{Be}$  flux.

## 4 Conclusions

The SK measurements of the energy spectrum and of day/night and seasonal variations of the neutrino flux have not realized, so far, any “smoking gun” in the study of the solar neutrino problem. Nevertheless these measurements provide significant information, since independent from theoretical models. Their use, combined with a proper treatment of all the different rate measurements allows an almost direct determination of the preferred values of the  $^8\text{B}$  and  $^7\text{Be}$  solar neutrino fluxes. In turn these values can be compared with the SSM expectations.

This comparison at present is encouraging but far from conclusive, as illustrated in fig 1. In particular, also in view of fig. 2, it makes it clear how premature it is to select one specific pattern of neutrino oscillations to explain the solar neutrinos. Nevertheless, data expected in the near future especially from SNO or from Borexino can turn this comparison into a convincing proof of solar neutrino oscillations and can also provide, at the same time, an independent validation of the SSM from neutrino physics.

**Acknowledgments** We thank Andrea Romanino for useful discussions.

## A Details of the computation

The energy spectra for the independent components of the solar neutrino flux have been obtained from [16]. The neutrino production has been averaged for each flux component over the position in the sun as predicted in [5, 16]. This averaging does not give significant corrections. MSW oscillations inside the sun have been taken

into account in the following way. The  $3 \times 3$  density matrix  $\rho_S$  for neutrinos exiting from the sun is computed using the Landau-Zener approximation with the level-crossing probability appropriate for an exponential density profile [17, 18]. The density profile has been taken from [16] and is quasi-exponential: small corrections to  $\rho_S$  have been approximately included. Oscillation effects outside the sun are described by the evolution matrix  $U$ , so that at the detection point  $\rho_E = U\rho_S U^\dagger$ . In particular, earth regeneration effects have been computed numerically using the mantle-core approximation for the earth density profile. We have used the tree level Standard Model expression for the neutrino/electron cross section at SK. The CC and NC cross sections at SNO have been taken from [19]. The experimental resolution at SK and SNO has been included as suggested in [19].

The total neutrino rates measured with the three kind of experimental techniques are [1, 2, 3, 4]

$$\Phi_{\text{Cl}}|_{\text{exp}} = (2.56 \pm 0.22) 10^{-36} \text{s}^{-1} \quad (3a)$$

$$\Phi_{\text{Ga}}|_{\text{exp}} = (74.7 \pm 5) 10^{-36} \text{s}^{-1} \quad (3b)$$

$$\Phi_{\text{SK}}|_{\text{exp}} = (2.40 \pm 0.08) \cdot 10^6 \text{cm}^{-2} \text{s}^{-1} \quad (3c)$$

having combined systematic errors in quadrature with statistical errors. The SuperKamiokande experimentalists give directly the value of the flux they measure. The other experiments involve more uncertain neutrino cross sections and prefer to give the frequency of events measured per target atom in their detector.

The solar model independent SK data included in the fit are: the energy spectrum of the recoil electrons (divided in 18 energy bins between 5.5 MeV and 15 MeV) and the total flux measured at SK during the day and during five night bins (defined according to the value of the cosine of the zenith angle) [2, 4]. The SK collaboration can include in their fit data about the zenith angle variation of the recoil electron spectrum and exclude the old SMA at 95% C.L. With these unpublished data the standard and the SSM-independent SMA solution would be less attractive and fig. 1 would show a more neat separation into two distinct regions.

## B Large $\Delta m_{12}^2$ and nu-factories

The standard interpretation of the solar neutrino anomaly is based on many experimental and theoretical ingredients. We have discussed how the SSM predictions can be tested. There is one other ingredient that could be not solidly founded and that has a significant impact on the final result [8, 15]. Only a single experiment, the Homestake one, has detected neutrinos with the Chlorine technique (with the other techniques, data come from two

water Cerenkov and two Gallium experiments). Furthermore Homestake is the only experiment that observes a rate different than one half of the SSM prediction in absence of oscillations, therefore excluding an energy-independent survival probability  $P_{ee}(E_\nu) \approx 1/2$ . This important conclusion could be the result of an under-estimation of the systematic error, that according to the Chlorine collaboration [1] is equal to the statistical error. It would be interesting to perform a direct calibration of the Chlorine detector [20].

$P_{ee}(E_\nu) \approx 1/2$  can be obtained with  $\theta_{12} \approx \pi/4$  and  $\Delta m_{12}^2 \gtrsim 10^{-4} \text{ eV}^2$ . This oscillation pattern has no problems with the recent SuperKamiokande data so that, even in a standard analysis, it is no longer significantly worse than the new best fits.

The KamLand experiment [21] will test the LMA region looking at disappearance of  $\bar{\nu}_e$  reactor neutrinos. If  $\Delta m_{12}^2$  and  $\theta_{12}$  lie inside the LMA region, KamLand can accurately measure them [22]. If instead  $\Delta m_{12}^2 \gtrsim 2 \cdot 10^{-4} \text{ eV}^2$ ,  $\bar{\nu}_e$  oscillations are averaged so that a measurement of  $\Delta m_{12}^2$  needs a good energy resolution, a precise knowledge of the un-oscillated spectra, high statistics and low background. Assuming that these conditions can be satisfied, fig. 6 shows the accuracy at which KamLand can measure few values of  $\Delta m_{12}^2$  and  $\theta_{12}$  (represented by the dots) after three years of running (i.e. with 2400 events if no oscillation occur). If  $\Delta m_{12}^2$  is too large statistical fluctuations often lead to discrete ambiguities in its determination. A reactor experiment with a *shorter* baseline would not have this problem.

Here, we study the impact of a large  $\Delta m_{12}^2$  at a neutrino factory [23]. Due to the high beam purity, a neutrino factory will allow to study  $\nu_e \rightarrow \nu_\mu$  and  $\bar{\nu}_e \rightarrow \bar{\nu}_\mu$  oscillations down to small values of the oscillation probability. Extensive studies [23, 24] have determined the optimal energy and pathlength that give the maximal sensitivity to a small  $\theta_{13}$ . If  $\theta_{13} = 0$  ‘solar’ oscillations give effects  $\propto (\Delta m_{12}^2)^2$  that can be seen at a neutrino factory if  $\Delta m_{12}^2 \gtrsim 2.5 \cdot 10^{-4} \text{ eV}^2$ . With a non-zero  $\theta_{13}$  and even for values of  $\Delta m_{12}^2$  inside the LMA region, ‘solar’ effects  $\propto \Delta m_{12}^2$  have a significant impact on  $\theta_{13}$  measurements at a neutrino factory [24].

The most promising observable for discovering  $\nu_e \rightarrow \nu_\mu$  oscillations is given by  $\mu^-$  appearance at a relatively short baseline  $L \approx 700 \text{ km}$ . The number  $N(\mu_-)$  of  $\mu^-$  events produced by both ‘solar’ and ‘atmospheric’ oscillations can be approximated by treating  $\theta_{13}$  and  $\Delta m_{12}^2$  effects as perturbations. This gives<sup>†</sup>  $P(\nu_e \rightarrow \nu_\mu) \approx$

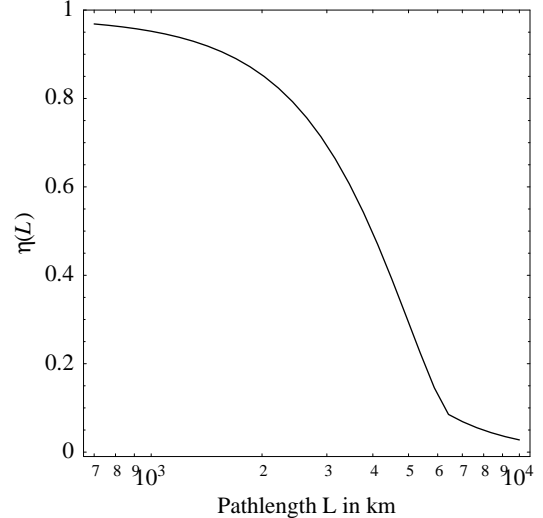


Figure 5: *Suppression of  $\Delta m_{12}^2$  oscillations due to matter effects as function of the pathlength  $L$*

$|\Delta_{e\mu}^{\text{eff}} L / 2E_\nu|^2$  and

$$N(\mu^-) \approx \frac{N_\mu N_{\text{kt}} \epsilon}{10^{21}} \frac{E_\mu}{70 \text{ GeV}} \left| \frac{\Delta_{e\mu}^{\text{eff}}}{10^{-5} \text{ eV}^2} \right|^2 \quad (4)$$

where  $N_\mu$  is the number of  $\mu^+$  decays occurring in the straight section of the storage ring pointing towards the detector,  $E_\mu \sim (20 \div 50) \text{ GeV}$  is the  $\mu^+$  energy,  $N_{\text{kt}}$  is the size of the detector in kilo tons,  $\epsilon$  is the efficiency for the detection of  $\mu^-$ . Using the parameterization (1)

$$\begin{aligned} \Delta_{e\mu}^{\text{eff}} \equiv & e^{i\phi} \Delta m_{12}^2 c_{23} c_{13} c_{12} s_{12} \frac{e^{iAL/2E} - 1}{iAL/2E} + \\ & + (\Delta m_{13}^2 - \Delta m_{12}^2 s_{12}^2) s_{13} c_{13} s_{23} \frac{e^{-iA'L/2E} - 1}{-iA'L/2E} \end{aligned}$$

where  $A = 2\sqrt{2}N_e G_F E_\nu$ ,  $A' = \Delta m_{13}^2 - A$ ,  $c_{ij} \equiv \cos \theta_{ij}$  and  $s_{ij} \equiv \sin \theta_{ij}$ . If the phase factors are large one should average  $N(\mu^-)$  over the neutrino spectrum, otherwise one can set  $E_\nu \approx E_\mu$ . For small  $L$  (in practice for  $L \lesssim 700 \text{ km}$ )  $\Delta_{e\mu}^{\text{eff}}$  reduces to the  $e\mu$  element of the neutrino squared mass matrix. Assuming a short baseline,  $\Delta m_{12}^2 \ll \Delta m_{13}^2$ ,  $\theta_{12} \approx \theta_{23} \approx \pi/4$  and  $\theta_{13} \ll 1$

$$\Delta_{e\mu}^{\text{eff}} \approx \theta_{13} \frac{\Delta m_{13}^2}{\sqrt{2}} + e^{i\phi} \frac{\Delta m_{12}^2}{2\sqrt{2}}$$

we clearly see in an analytical way how significant  $\Delta m_{12}^2$  oscillations can be. An analogous approximation holds for  $\bar{\nu}_e \rightarrow \bar{\nu}_\mu$  signals.

At baselines  $L \gtrsim 10^3 \text{ km}$  matter effects become significant. Using eq. (4), the number of events due to  $\Delta m_{12}^2$  oscillations only can be written as its value at  $L = 0$

<sup>†</sup>Using the formula  $e^{M+\epsilon} = e^M (1 + \int_0^1 e^{-xM} \cdot \epsilon \cdot e^{xM} dx + \mathcal{O}(\epsilon^2))$ .

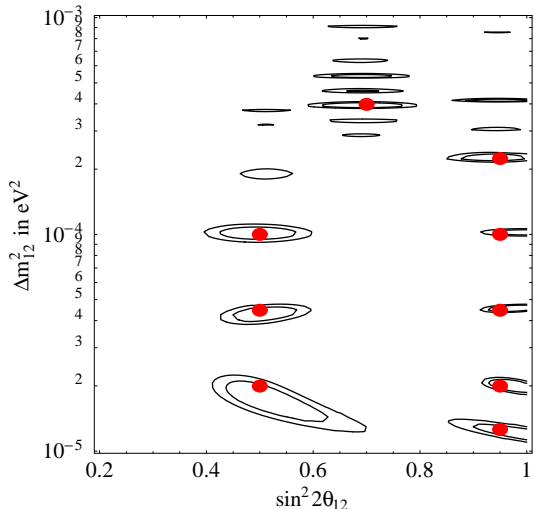


Figure 6: Few fits at 90% and 99% C.L. of simulated KamLand data after three years of running.

multiplied by the function

$$\eta(L) = \frac{\sin^2 x}{x^2} < 1, \quad x \equiv \frac{N_e G_F L}{\sqrt{2}}$$

which exact numerical value is plotted in fig. 5. Therefore a short baseline  $L \approx 700$  km is optimal for discovering  $\Delta m_{12}^2$  effects.

By performing a global fit of simulated nu-factory data we find that it will be difficult to distinguish  $\Delta m_{12}^2$  effects from  $\theta_{13}$  effects at a good C.L. by comparing data taken at different pathlengths and/or different neutrino energies, as suggested in [24]. For certain values of the CP violating phase a comparison between  $\nu_e \rightarrow \nu_\mu$  and  $\bar{\nu}_e \rightarrow \bar{\nu}_\mu$  rates allows a better discrimination. Such ‘precision studies’ are statistically significant only with a sufficient number of events. For example, observing few events only would not allow to say if they are due to a  $\theta_{13} \approx 0.007$  around its nominal sensitivity, or due to a  $\Delta m_{12}^2 \approx 3 \cdot 10^{-4} \text{ eV}^2$ . In conclusion, if  $\Delta m^2 \gtrsim 2 \cdot 10^{-4} \text{ eV}^2$  so that KamLand cannot measure it, an accurate measurement of  $\Delta m^2$  cannot even be obtained with a neutrino factory: a new reactor experiment with intermediate baseline  $\sim 10$  km would be necessary.

If KamLand will give a precise measurement of  $\Delta m_{12}^2$  free from discrete ambiguities (this could not be the case if  $\Delta m_{12}^2 \gtrsim 2 \cdot 10^{-4} \text{ eV}^2$ ), by combining KamLand data with nu-factory data one can usually obtain a satisfactory fit of  $\theta_{13}$  and of the CP violating phase.

## References

[1] The results of the Homestake experiment are reported in B.T. Cleveland et al., *Astrohys. J.* **496** (1998) 505.

[2] The SuperKamiokande collaboration, *Phys. Rev. Lett.* **82** (1999) 2430, *Nucl.Phys.Proc.Suppl* **77** (1999) 35, *Nucl.Phys.Proc.Suppl* **81** (2000) 133.

[3] Gallex collaboration, *Phys. Lett.* **B447** (1999) 127; SAGE collaboration, *Phys. Rev.* **C60** (1999) 055801;

[4] Talks by E. Bellotti, V. Gavrin and Y. Suzuki at the conference ‘Neutrino 2000’, Sudbury, Canada, June 2000.

[5] J.N. Bahcall, S. Basu and M.H. Pinsonneault, *Phys. Lett.* **B433** (1998) 1 (*astro-ph/9805135*) and refs therein.

[6] G.L. Fogli, E. Lisi, D. Montanino, A. Palazzo, *Phys. Rev.* **D62** (2000) 113003 (*hep-ph/0008012*); M.C. Gonzales-Garcia and C. Peña-Garay, *hep-ph/0009041*.

[7] LSND collaboration, *Phys. Rev.* **C54** (1996) 2685 and *Phys. Rev.* **C58** (1998) 2489.

[8] R. Barbieri et al., *J.hep* **12** (1998) 017 (*hep-ph/9807235*).

[9] N. Hata and P. Langacker, *Phys. Rev.* **D52** (1995) 420 (*hep-ph/9409372*); N. Hata and P. Langacker, *Phys. Rev.* **D56** (1997) 6107 (*hep-ph/9705339*); V. Castellani et al., *Phys. Rep.* **281** (1997) 309 (*astro-ph/9606180*).

[10] The CHOOZ collaboration, *Phys. Lett.* **B466** (1999) 415 (*hep-ex/9907037*). See also The Palo Verde experiment, *Phys. Rev. Lett.* **84** (2000) 3764 (*hep-ex/9912050*).

[11] G.L. Fogli, E. Lisi, D. Montanino, *Phys. Rev.* **D54** (1996) 2048 (*hep-ph/9605273*); A. de Gouvea, A. Friedland, H. Murayama, *Phys. Lett.* **B490** (2000) 125 (*hep-ph/0002064*).

[12] G.L. Fogli, E. Lisi, D. Montanino and A. Palazzo, *Phys. Rev.* **D61** (2000) 073009 (*hep-ph/9910387*).

[13] J.N. Bahcall, P.I. Krastev, A.Yu. Smirnov, *Phys. Rev.* **D62** (2000) 093004 (*hep-ph/0002293*); M. Maris, S.T. Petcov, *Phys. Rev.* **D62** (2000) 093006 (*hep-ph/0003301*). J.N. Bahcall, P.I. Krastev, A.Yu. Smirnov, *hep-ph/0006078*.

[14] M.C. Gonzales-Garcia and C. Peña-Garay, *hep-ph/0011245*.

[15] A. Strumia, *J.hep* **04** (1999) 026 (*hep-ph/9904245*).

[16] J.N. Bahcall, [www.sns.ias.edu/~jnb](http://www.sns.ias.edu/~jnb).

[17] L. Wolfenstein, *Phys. Rev.* **D17** (1978) 2369; S.P. Mikheyev and A. Yu Smirnov, *Sovietic Jour. Nucl. Phys.* **42** (1986) 913.

[18] S. Parke, *Phys. Rev. Lett.* **57** (1986) 1275; P. Pizzochero, *Phys. Rev.* **D36** (1987) 2293; S.T. Petcov, *Phys. Lett.* **B200** (1998) 373; for a review see T.K. Kuo and J. Pantaleone, *Rev. Mod. Phys.* **61** (1989) 937.

[19] J.N. Bahcall and E. Lisi, *Phys. Rev.* **D54** (1996) 5417.

[20] Talk by K. Lande at the conference ‘Neutrino 2000’, Sudbury, Canada, June 2000.

[21] KamLAND Collaboration, *Nucl.Phys.Proc.Suppl.* **87** (312) 2000, [www.awa.tohoku.ac.jp/html/KamLAND/index.html](http://www.awa.tohoku.ac.jp/html/KamLAND/index.html)

[22] V. Barger, D. Marfatia and B.P. Wood, *hep-ph/0011251*.

[23] S. Geer, *Phys. Rev.* **D57** (1998) 6989 (*hep-ph/9712290*) and erratum, *Phys. Rev.* **D59** (1999) 039903; A. De Rújula, M.B. Gavela and P. Hernández, *Nucl. Phys.* **B547** (1999) 21 (*hep-ph/9811390*); C. Albright et al., Report to the Fermilab directorate, *hep-ex/0008064* and refs therein.

[24] see e.g. M. Freund, M. Lindner, S.T. Petcov, A. Romanino, *Nucl. Phys.* **B578** (2000) 27 (*hep-ph/9912457*); A. Cervera et al., *Nucl. Phys.* **B579** (2000) 17 (*hep-ph/0002108*).

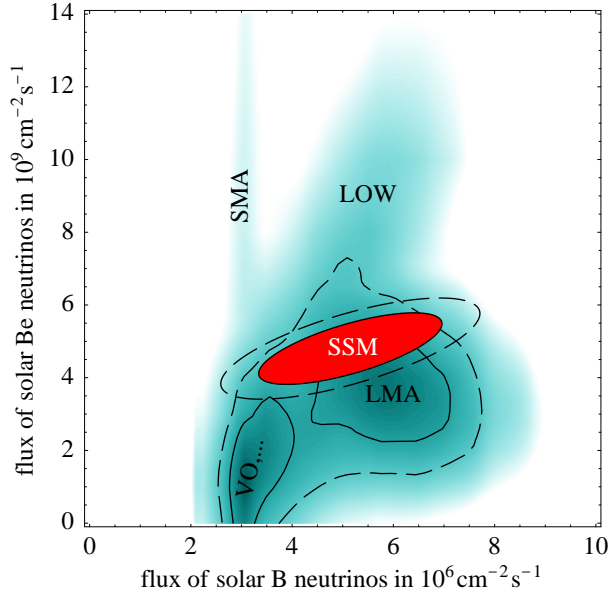


Figure 7: *Fig. 1 updated including the SNO CC result: best fit, at 90% CL (continuous line) and 99% CL (dashed line), of the neutrino solar fluxes compared with SSM theoretical predictions.*

## 5 Addendum: SNO CC results

In this addendum, we update our results by adding the first SNO [1] data. The SK collaboration published the day + night spectral data [2] as 19 + 19 energy bins, so that we can now include this information in the fit. We also explicitly included the CHOOZ data [10], that disfavour values of  $\Delta m_{12}^2$  above  $0.7 \cdot 10^{-3} \text{ eV}^2$  for large mixing  $\theta_{12} \sim \pi/4$ . Finally, we improved the numerical accuracy of our computation, and extended it to include vacuum oscillations [3].

As pointed out in section 3, the measurement of the NC/CC ratio alone was expected to discriminate between LMA and SMA. The measured value happens to fall into case 4. (cases 3. and 5. are not significantly disfavoured). Therefore the SMA region is now strongly disfavoured, even from a solar-model-independent point of view. Furthermore, the solar-model-independent LMA region (case 5.) no longer gives a best  $\chi^2$  significantly lower than the standard fit. These results are confirmed by an updated analysis, as shown in fig. 7 and 8.

In fig. 7 we show the updated fit of the solar neutrino fluxes. Values of the  $^8\text{B}$  flux detectably different from the SSM prediction no longer give good fits. On the contrary, a discrepancy between the  $^7\text{Be}$  flux and its SSM prediction could still have significant effects. The best-fit region at 90% CL in fig. 7 is composed by two disjoint regions. The one with smaller fluxes is obtained

from vacuum oscillations (but can also be obtained with LMA, LOW, SMA oscillations with a worse CL). The one with larger fluxes is obtained from LMA oscillations.

In fig. 8 we show the updated global fits for the oscillation parameters: fig. 8a shows a standard fit, while fig. 8b is the solar model independent fit described in section 2. In fig. 8c we perform a standard fit, but dropping the uncalibrated Chlorine rate from the fit. The results of fig.s 8a,b,c are quite similar: more or less acceptable fits can be obtained for a large range of  $\Delta m^2$  and large mixing angle, while the SMA solution is always disfavoured.

Finally, we mention another important aspect of solar model independent analyses. It is sometimes said that it is useless to measure the Gallium rate with an error much smaller than the solar model uncertainty. As explained in section 2 and illustrated in fig.s 2, this is not true. Fig.s 2 in fact shows that the amount of information that can be extracted in a solar model independent way from the solar rates is today limited by the accuracy of the Chlorine experiment. This limitation will disappear when Borexino will measure the  $^7\text{Be}$  flux. Fig.s 8 show that solar model independent considerations already now give useful informations on the oscillation parameters.

## References

- [1] The SNO collaboration, *nucl-ex/0106015*. For global post-SNO analyses of solar neutrino data see G.L. Fogli, E. Lisi, D. Montanino, A. Palazzo, *hep-ph/0106247*; J.N. Bahcall, M.C. Gonzalez-Garcia, C. Peña-Garay, *hep-ph/0106258*; A. Bandyopadhyay, S. Choubey, S. Goswami, K. Kar, *hep-ph/0106264*; the addendum to P. Creminelli, G. Signorelli, A. Strumia, *hep-ph/0102234* (not present in the published version).
- [2] The SuperKamiokande collaboration, *hep-ex/0103032*.
- [3] Values of  $\Delta m^2 < 10^{-8} \text{ eV}^2$  were not considered in the pre-SNO version of the paper. For useful studies of matter effects in such regions see G.L. Fogli, E. Lisi, D. Montanino, A. Palazzo, *Phys. Rev. D* **62** (2000) 113004 (*hep-ph/0005261*); E. Lisi, A. Marrone, D. Montanino, A. Palazzo, S.T. Petcov, *Phys. Rev. D* **63** (2001) 93002 (*hep-ph/0011306*) and ref.s therein.

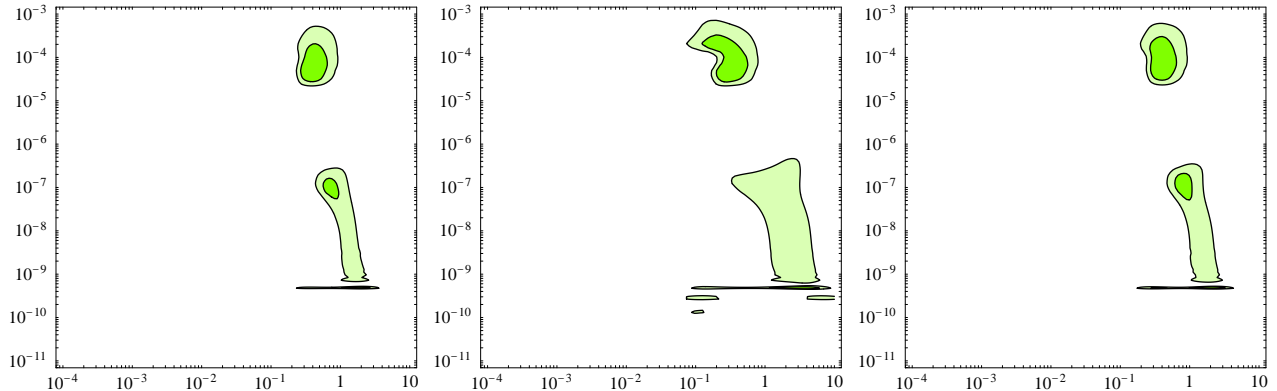


Figure 8: *Global fits of solar data (updated including SNO CC data) at 90, 99% CL in the  $(\tan^2 \theta_{12}, \Delta m_{12}^2 / \text{eV}^2)$  plane: (a) standard fit; (b) solar model independent fit; (c) standard fit dropping the uncalibrated Chlorine data.*

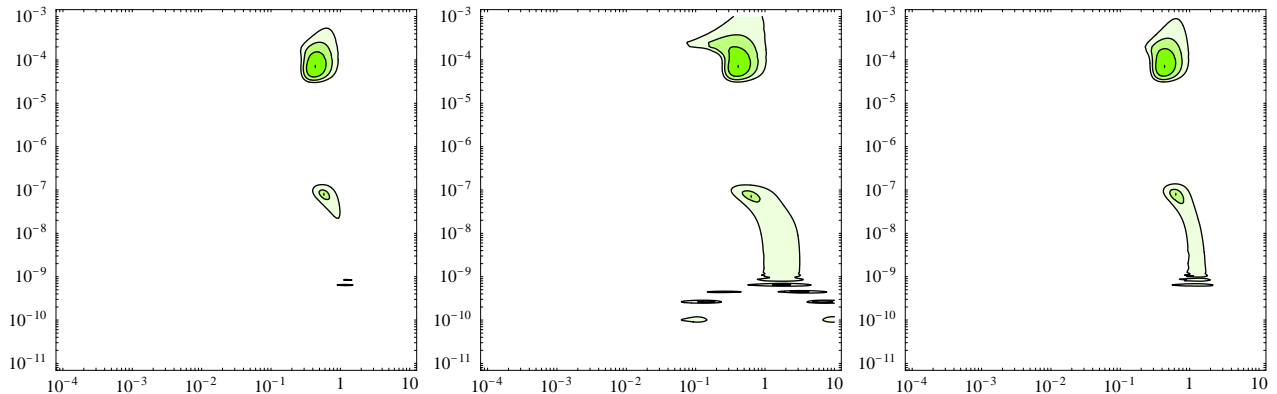


Figure 9: *Global fits of solar data (updated including SNO NC data) at 90, 99, 99.9% CL in the  $(\tan^2 \theta_{12}, \Delta m_{12}^2 / \text{eV}^2)$  plane: (a) standard fit; (b) solar model independent fit; (c) standard fit dropping the uncalibrated Chlorine data.*

## 6 Addendum: SNO NC results

In this addendum, we update our results by adding the latest SAGE, GNO and SK data and the SNO day/night energy spectrum [1]. As explained in the SNO paper, the SNO spectrum allows to extract its NC, CC and ES contributions. For example, assuming energy-independent oscillations between active neutrinos, our reanalysis of SNO data gives

$$\Phi_{\text{NC}} = \Phi_{\text{sB}} = (5.2 \pm 0.5) 10^6 / \text{cm}^2 \text{s}, \quad (5a)$$

$$\Phi_{\text{CC}} = P_{ee} \Phi_{\text{sB}} = (1.76 \pm 0.08) 10^6 / \text{cm}^2 \text{s}. \quad (5b)$$

(the errors are somewhat anti-correlated).<sup>¶</sup>

<sup>¶</sup>Our reanalysis slightly differs from the corresponding SNO analysis in [1]. SNO extracts from all data (energy and zenith-angle spectra) the CC, NC and ES components. We instead extract the CC, NC components from the energy spectrum, assum-

As expected, new data have a significant impact on the oscillation fit [3]. In fig. 9 we show the updated global fits for the oscillation parameters: fig. 9a shows a standard fit, while fig. 9b is the solar model independent fit described in section 2. In fig. 9c we perform a standard fit, but dropping the uncalibrated Chlorine rate from the fit. The results of figs 9a,b,c are quite similar: more or less acceptable fits can be obtained for a large range of  $\Delta m^2$  and for large mixing angle, while the SMA solution is always incompatible with data at about  $5\sigma$  level. In all analyses LMA oscillations give a better fit than LOW and (Q)VO oscillations. In figs 9a,b,c we

ing the standard relation  $\Phi_{\text{ES}} \approx \Phi_{\text{CC}} + 0.15\Phi_{\text{NC}}$  (the ES rate have also been accurately measured by SK). We take into account systematic errors and backgrounds as described by SNO [1], as well as the theoretical uncertainty on the Boron energy spectrum (that also affects other solar neutrino experiments). See [2] for a useful discussion of these issues.

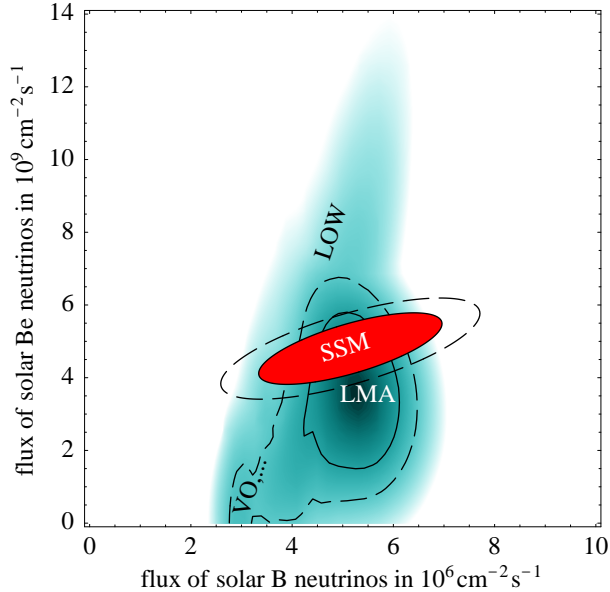


Figure 10: *Fig.s 1, 7 updated including the SNO NC result: best fit, at 90% CL (continuous line) and 99% CL (dashed line), of the neutrino solar fluxes compared with SSM theoretical predictions.*

have not included the CHOOZ bound, in order to show that  $\Delta m^2 \gtrsim 10^{-3} \text{ eV}^2$  is now disfavoured by solar data.

In fig. 10 we show the Boron and Beryllium fluxes, as extracted from the solar neutrino data without assuming solar model predictions for these fluxes, and assuming that the solar anomaly is due to  $\nu_e \rightarrow \nu_{\mu,\tau}$  oscillations.

Within this framework, SNO has measured the Boron flux through NC scattering, finding a value in agreement with solar model predictions. A much larger Boron flux was already excluded in our previous analysis (see figures 1 and 7) because it would need a small and energy-independent survival probability  $P_{ee}(E_\nu)$ , that cannot be obtained by oscillations.

In view of this experimental progress, one can study if new significant information, e.g. about the CNO and  $pp$  fluxes, can now be extracted from a more general analysis. Since the results are not very interesting, we just briefly describe their main features. Only two kind of experiments, Gallium and Chlorine, have measured low-energy neutrino fluxes. Therefore, one can think of extracting the values of two of these fluxes at most. The Chlorine experiment is not very sensitive to low energy neutrinos: after subtracting the  $\sim 80\%$  Boron contribution, as measured by SNO via CC, the residual Chlorine rate is just about  $2\sigma$  above zero.

A first interesting question is: do solar neutrino data discriminate between CNO and  ${}^7\text{Be}$  neutrinos? We find

that equally good fits are obtained in the extreme limits of vanishing CNO or  ${}^7\text{Be}$  flux. Therefore fig. 10, where the Be flux is studied, provides all the significant information on Be and CNO fluxes, and implies that their sum is at most 2 times larger than solar model predictions. This means that the solar luminosity constraint fixes the  $pp$  flux to be around its solar model value.

A second issue is: what is it possible to say on the  $pp$  flux, without imposing the luminosity constraint (and of course without assuming the solar model predictions for the other fluxes). The relatively more interesting result is that the  $pp$  flux cannot be zero, as can be seen by comparing the Gallium, Chlorine and SNO CC rates.

Ref. [2] finds that the pulls between solar model predictions and their best-fit values (as obtained from a global oscillation fit that *includes* these predictions) are small. Note, however, that solar models are not confirmed in this way. While a large pull would signal a problem, a small pull is obtained in two cases: when the experimental determination agrees with the prediction (this happens in the case of the Boron flux) but also when the experimental error is much larger than the theoretical error (this roughly happens for all other fluxes). Looking at pulls only, one cannot discriminate these two extreme cases. In order to test predictions one must extract the predicted quantities (e.g. the B and Be fluxes in fig. 10, more generically any other ‘systematics’ relevant for solar data) by fitting the data *without* assuming the predictions under examination.

## References

- [1] The SNO collaboration, *nucl-ex/0204008 and nucl-ex/0204009*. See also “HOWTO use the SNO solar neutrino spectral data”, [www.sno.phy.queensu.ca/sno](http://www.sno.phy.queensu.ca/sno). The SAGE collaboration, *astro-ph/0204245*. GNO data have been reported by T. Kirsten, talk at the Neutrino 2002 conference, transparencies available at the internet address [neutrino2002.ph.tum.de](http://neutrino2002.ph.tum.de). We use as Gallium solar rate the averaged result of all (older and newer) Gallium experiments. The Super-Kamiokande collaboration, *hep-ex/0205075*.
- [2] G.L. Fogli et al., *hep-ph/0206162*.
- [3] See e.g. A. Bandyopadhyay et al., *hep-ph/0203169*; M. Maris, S.T. Petcov, *hep-ph/0201087*. For recent standard analyses of solar data see V. Barger et al., *hep-ph/0204253*; P. Creminelli et al., *hep-ph/0102234* (updated on 22 Apr 2002 including the SNO NC and day/night results); A. Bandyopadhyay et al., *hep-ph/0204286*; J.N. Bahcall et al., *hep-ph/0204314*; P. Aliani et al., *hep-ph/0205053*; P.C. de Holanda et al., *hep-ph/0205241*; C. Cattadori et al., *hep-ph/0205261*. See also the SK and SNO papers in [1], and [2].